DOI: 10.1002/ejoc.201000579

Competitive Formation of β-Enaminones and 3-Amino-2(5*H*)-furanones from the Isoxazolidine System: A Combined Synthetic and Quantum Chemical Study

Daniela Iannazzo,*[a] Elisa Brunaccini,[a] Salvatore V. Giofrè,[a] Anna Piperno,[a] Giovanni Romeo,[a] Simone Ronsisvalle,[b] Maria A. Chiacchio,[c] Giuseppe Lanza,*[c] and Ugo Chiacchio[c]

Dedicated to Professor Saverio Florio on the occasion of his 70th birthday

Keywords: 1,3-Dipolar cycloaddition / Density function calculations / Isoxazolidines / β-Enaminones / 2(5*H*)-Furanones

Treatment of 3-alkoxycarbonyl-4-acyl- or 3,4-dialkoxycarbonyl-substituted isoxazolidines with a mild base, such as tetrabutylammonium fluoride, affords β-enaminones and/or 3-methylamino-2(5*H*)-furanones according to the nature of the substituents at C^4 and C^5. Two alternative mechanisms (lactonization and retro-aldolization) have been rationalized by DFT quantum chemical methods. Any realistic theoretical modeling requires the explicit inclusion of countercation and solvent effects.

Introduction

Isoxazolidines, easily accessible through the 1,3-dipolar cycloaddition of nitrones to substituted alkenes are valuable synthons for the production of simple and complex molecules.[1] The ring opening of these heterocycles allows a facile access to a variety of functionalized intermediates, such as 1,3-amino alcohols, α,β-enones, tetrahydro-1,3-oxazines, N-substituted hydroxylamines, 1,3-amino-ketones, polysubstituted allylic alcohols, and γ- and δ-lactams (Figure 1).[2] In particular, the basic treatment of isoxazolidines suitably activated at the 3-position of the pentatomic ring has been exploited for a general synthetic approach to 3-alkylamino-2(5*H*)-furanones, versatile synthons for β-lactams.[3] Thus, 3-alkoxycarbonyl-substituted isoxazolidines **1** undergo rearrangement to furanones **2** after treatment with NaH at room temperature (Figure 2).[4] Recently, the chemical conversion of 3-alkoxycarbonyl-4-acyl- or 3,4-dialkoxycarbonyl-substituted isoxazolidines **3** to 3-alkylamino-2(5*H*)-furanones **4** has been performed by using a mild base, such as tetrabutylammonium fluoride (TBAF), in 75–85% yield. Compounds **4**, which can be considered as diketo acid cyclic analogues, have shown very interesting biological properties as inhibitors of subgenomic hepatitis C virus RNA replication.[5] The driving force for this kind of rearrangement is represented by the low critical energy required to induce an anionic centre at the C^3 position of the isoxazolidine nucleus, which promotes the ring opening of the heterocyclic system and the subsequent intramolecular lactonization.[4,5]

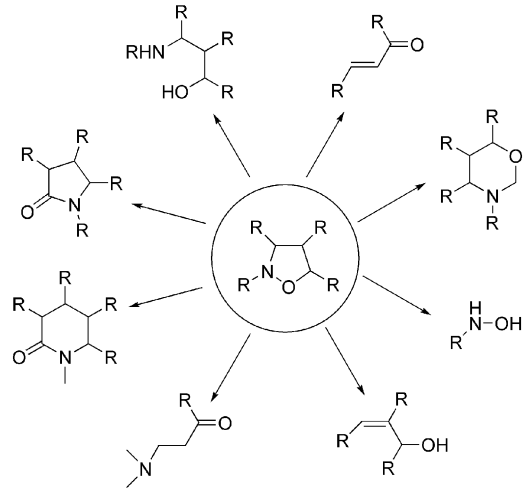

Figure 1. Ring-opening reactions of isoxazolidines.

[a] Dipartimento Farmaco-Chimico, Università di Messina, Via SS. Annunziata, 98168 Messina, Italy
Fax: +39-0906766562
E-mail: diannazzo@unime.it
[b] Dipartimento di Scienze Farmaceutiche, Università di Catania, Viale A. Doria, 6 95125 Catania, Italy
Fax: +39-095222239
[c] Dipartimento di Scienze Chimiche, Università di Catania, Viale A. Doria 6, 95125 Catania, Italy
Fax: +39-095580138
E-mail: glanza@unict.it

Supporting information for this article is available on the WWW under http://dx.doi.org/10.1002/ejoc.201000579.

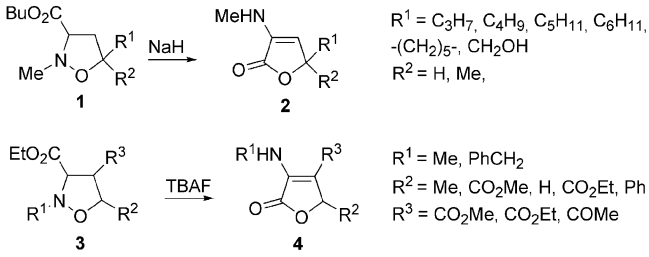

Figure 2. Chemical conversion of isoxazolidines **1** and **3** to 3-methylamino-2(5*H*)-furanones **2** and **4**.

In this paper, a different rearrangement route has been highlighted that leads to the formation of β-enaminones of type **5** valuable intermediates for the synthesis of heterocycle compounds.[6] This new reaction pathway competes with the process leading to compounds **4**, according to the nature of the substituents at C^4 and C^5 (Figure 3). We report here the mechanistic rationalization of this new reaction pathway together with the computational study supporting the suggested rearrangement. DFT quantum chemical calculations have allowed us to understand the factors that ultimately control the competitive reaction routes.

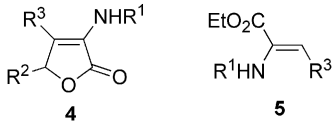

Figure 3. 3-Alkylamino-2(5*H*)-furanones **4** and β-enaminones **5**.

Results and Discussion

Isoxazolidines **10**–**12** were prepared by the reaction of *C*-ethoxycarbonyl-*N*-methyl nitrone **6** with α,β-unsaturated compounds **7**–**9**. In particular, the cycloaddition of nitrone **6** with *trans* methyl cinnamate **7**, performed in toluene at 80 °C for 18 h, proceeded in high yield (85%) to give, in agreement with similar cycloaddition processes,[7] a mixture of *trans*/*cis* isomers **10a** and **10b** (Scheme 1, Table 1).

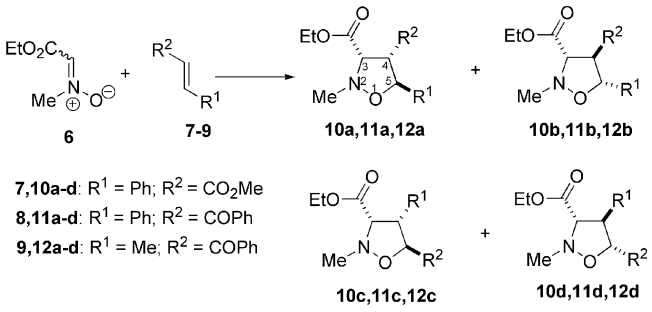

Scheme 1. Cycloaddition reaction of nitrone **6** with methyl cinnamate **7** and α,β-unsaturated ketones **8** and **9**.

No regioisomeric adducts (**10c**,**d**) were detected in the crude reaction mixture. The diastereoisomeric ratio of **10a**,**b** (4.5:1) was evaluated by the ^{1}H NMR spectrum of the crude reaction mixture; C^3–C^5 *trans* isomer **10a** was the major product of the cycloaddition. The stereochemical information present in the dipolarophile is completely retained in the cycloadducts and the relative stereochemistry at C^4 and C^5 in the formed isoxazolidine ring is predetermined by the alkene geometry. The stereochemical assignment has been assessed by NOE experiments (see the Supporting Information). The classic pericyclic reaction of **6** with α,β-unsaturated ketones **8** and **9** proceeded with low regio- and stereoselectivity. A better regiochemical control towards 4-acyl-substituted isoxazolidines **11a**,**b** and **12a**,**b** and increased yields were obtained by the use of the pinhole Lewis acid as a catalyst under mild conditions (Scheme 1).[8] Thus, in the presence of aluminum tris(2,6-diphenylphenoxide) (ATPH) catalyst, the crude reaction mixture shows the formation of at least three isomers consisting of one major product (49–62% of the total isomeric amount) besides other minor products (Table 1). All the isomers were separated and fully characterized (see the Exp. Section and Supporting Information).

Table 1. Cycloaddition between nitrone **6** and alkenes **7**–**9**.

Entry[a]	Alkene	Lewis acid	Product yield [%][b]	**a/b/c/d** (ratio)[c]
1	**7**	none	**10** (85)	4.5:1:0:0
2	**8**	none	**11** (20)	2:1:0.4:0.2
3	**8**	ATPH	**11** (86)	4:1:1:1
4	**9**	none	**12** (20)	2:2:1:0
5	**9**	ATPH	**12** (85)	4:1:0.5:0

[a] Entry 1 was carried out by using toluene at 80 °C, for 18 h; entries 2–5 were carried out by using dichloromethane at room temperature. [b] Isolated yield. [c] The relative ratio has been determined by ^{1}H NMR spectroscopy of the crude reaction mixture.

Treatment of isoxazolidines **11a**,**b** with TBAF in a 1:1 ratio led to the formation of compound **5b** as the exclusive product,[6] whereas, under the same experimental conditions, both compounds **10a**,**b** and **12a**,**b** afford a 80:20 mixture of 3-amino-2(5*H*)-furanones and β-enaminones (**4a**, **5a** from **10a**,**b** and **4b**, **5b** from **12a**,**b**; Scheme 2 and Table 2). The structure of the obtained β-enaminones **5a**,**b** has been assessed on the basis of spectrometric data (see the Supporting Information).

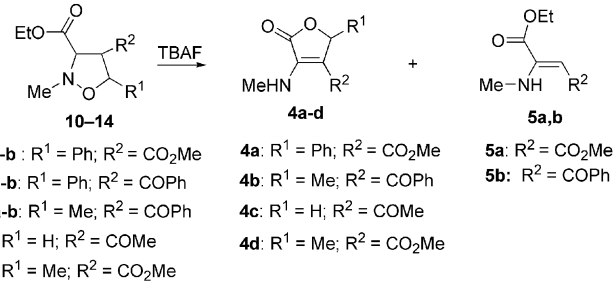

Scheme 2. Chemical conversion of isoxazolidines **10**–**14** towards 3-amino-2(5*H*)-furanones **4** and/or β-enaminones **5**.

Treatment of isoxazolidines **10**–**14** with 0.2 and 0.5 equivalents of TBAF led to a proportional decrease of the reaction yields, thus suggesting that the base is "captured" by final products and that the base does not work as a catalyst.

Table 2. Reaction of isoxazolidines **10**–**14** (**I**) with TBAF.

I	R^1	R^2	**4/5**
10	Ph	CO_2Me	20:80 [a]
11	Ph	COPh	0:100[a]
12	Me	COPh	20:80[a]
13	H	COMe	100:0[b]
14	Me	CO_2Me	100:0[b]

[a] Present work. [b] See ref.[5]

Theoretical Results

The new rearrangement pathway of the isoxazolidine nucleus can be rationalized as reported in Figure 4 (path B).

The carbanion **II**, formed by abstraction of the hydrogen atom at C^3 in **I**, undergoes a retroaldolization process, giving rise to compound **5** through extrusion of an aldehydic unit. This reaction route appears to compete with the rearrangement, previously reported, to furanones **4** (path A)[3–5] In fact, the same reaction, performed on differently substituted 3-ethoxycarbonyl isoxazolidines **13** and **14**, afforded furanones as the exclusive products[5] (Table 2). The competition between the two pathways leading to lactones **4a** and **4b** and β-enaminones **5a** and **5b** has been rationalized on the basis of theoretical calculations. By comparison, the results obtained for isoxazolidines **13** and **14** are also listed.[5] To better understand which factors control the different pathways, we investigated the two competitive reaction channels for **13** and **11**, chosen as model compounds, employing quantum chemical methods (see Computational Details in the Exp. Section). To study the entire reaction course it is necessary to include explicitly the TBAF activator and also the effects of the solvent (THF). However, to improve the computational performance, $(n\mathrm{Bu})_4N^+F^-$ was modeled by the tetramethylammonium fluoride $(CH_3)_4N^+F^-$. In the examined isoxazolidines (**I**), substituents at the C^4- and C^5-positions are in a *trans* configuration, whereas the substituent at C^3 can assume both a *cis* or a *trans* relationship with respect to C^4. Because of steric repulsions, (C^3–C^4)-*trans* structures, on the basis of the present calculations, have been found to be more stable than *cis* isomers (3.1 and 5.5 kcal/mol for **13-I** and **11-I** compounds, respectively, see Figure S1 in the Supporting Information). The energy of the more stable *trans* isomers was taken as a reference.

Several resonance structures and valence isomers (Figure 5) can be written for the carbanion **II**, arising from the treatment of isoxazolidines with TBAF, thus indicating a large negative charge delocalization that results in the weakening or strengthening of some bonds. Some of these struc-

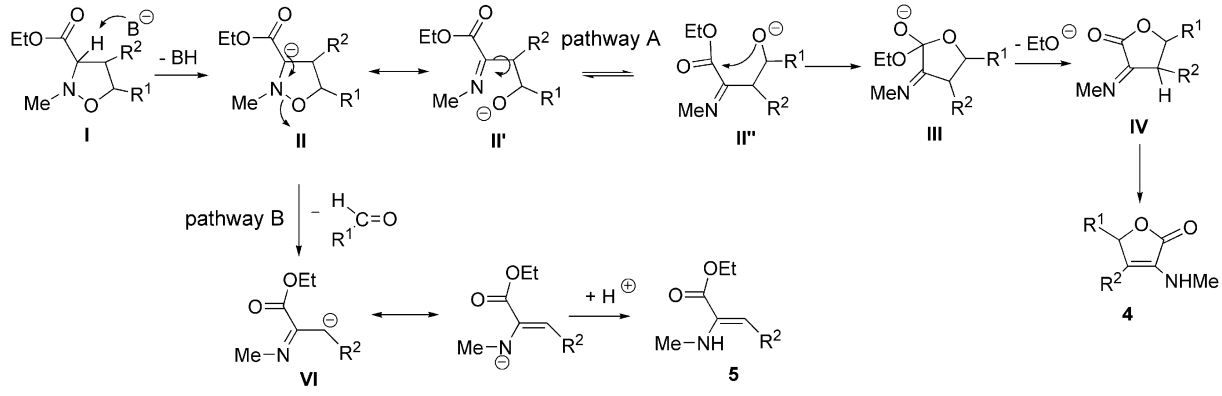

Figure 4. The rearrangement pathways of the isoxazolidine system.

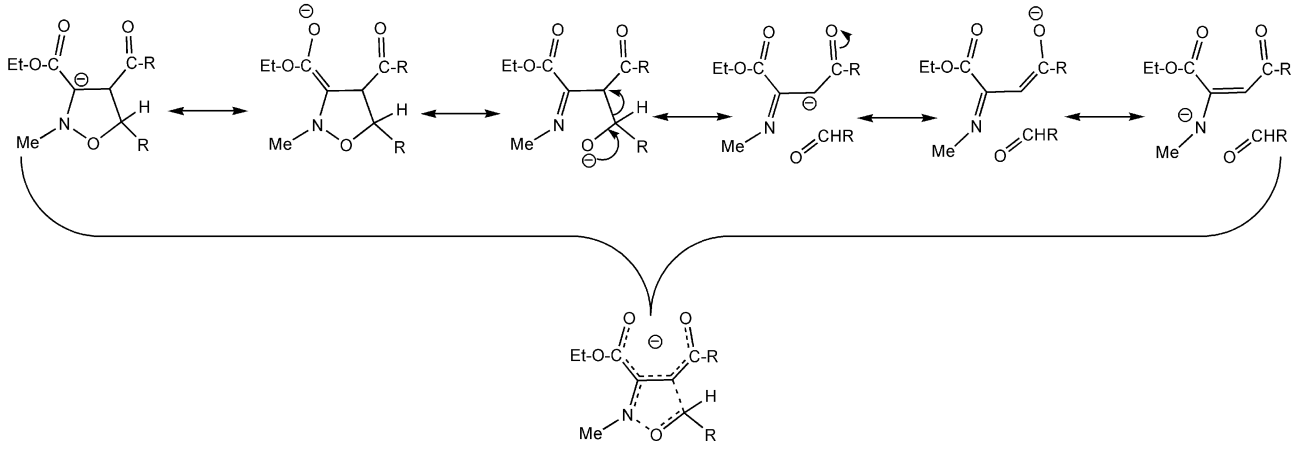

Figure 5. Resonance structures, valence isomer, and hypervalent structures of carbanion **II**.

tures suggest the possibility of ring degradation with aldehyde extrusion. Actually, for a "naked" carbanion, geometry optimizations result in a barrierless expulsion of formaldehyde or benzaldehyde. Only for the carbanion from **13** was it possible to find a high-energy minimum that maintains the isoxazolidine ring (see Figure S2 in the Supporting Information), whereas for compound **11** it was not possible to locate a stable carbanion of this kind. This consideration highlights two important aspects: there is an intrinsic tendency of the "naked" negatively charged isoxazolidine toward fragmentation and this tendency depends on the ring substituents.[9] In spite of this great tendency towards ring degradation, however, the latter is seldom experimentally observed.[4,5,7] This is likely due to a critical stabilization of the carbanion by the $(CH_3)_4N^+$ countercation (Figure 6).

The cation polarizes the negative ion and leads to a build-up of extra electronic density, that is, to very small covalency charge. In fact, the cation reduces the negative charge of the isoxazolidine ring [NBO charge on the $(CH_3)_4N$ fragment is 0.93 e.u.] and in turn prevents spontaneous retroaldolization. In this perspective, all the calculations for the two competitive reaction channels have been performed explicitly including countercation and solvent effects that greatly modulate the ionic interactions.[10]

By comparing metrical parameters of the isoxazolidine ring in the two analyzed contact ion pairs, a substantial elongation of the O^1–N^2 and C^4–C^5 bond lengths emerges and hence a bond weakening for **11-II** with respect to **13-II** (Figure 6). Conversely, the O^1–C^5 bond length indicates a bond strengthening in **11-II**. These data still point out a great tendency towards ring fragmentation of isoxazolidines that carry sterically hindered substituents. Another impor-

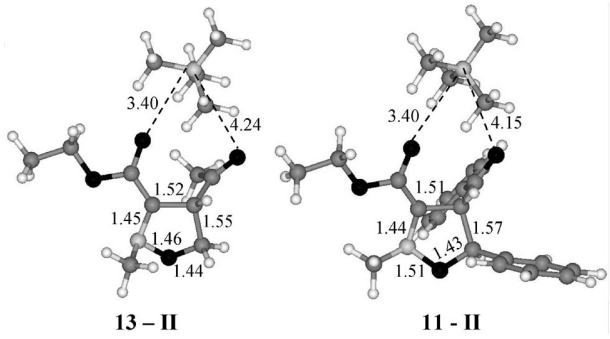

Figure 6. Most stable conformation of the contact cation–anion pairs (**II**) of the isoxazolidines **13** and **11**.

Figure 7. Localization of the countercation in the structure of **II′** (see Figure 4).

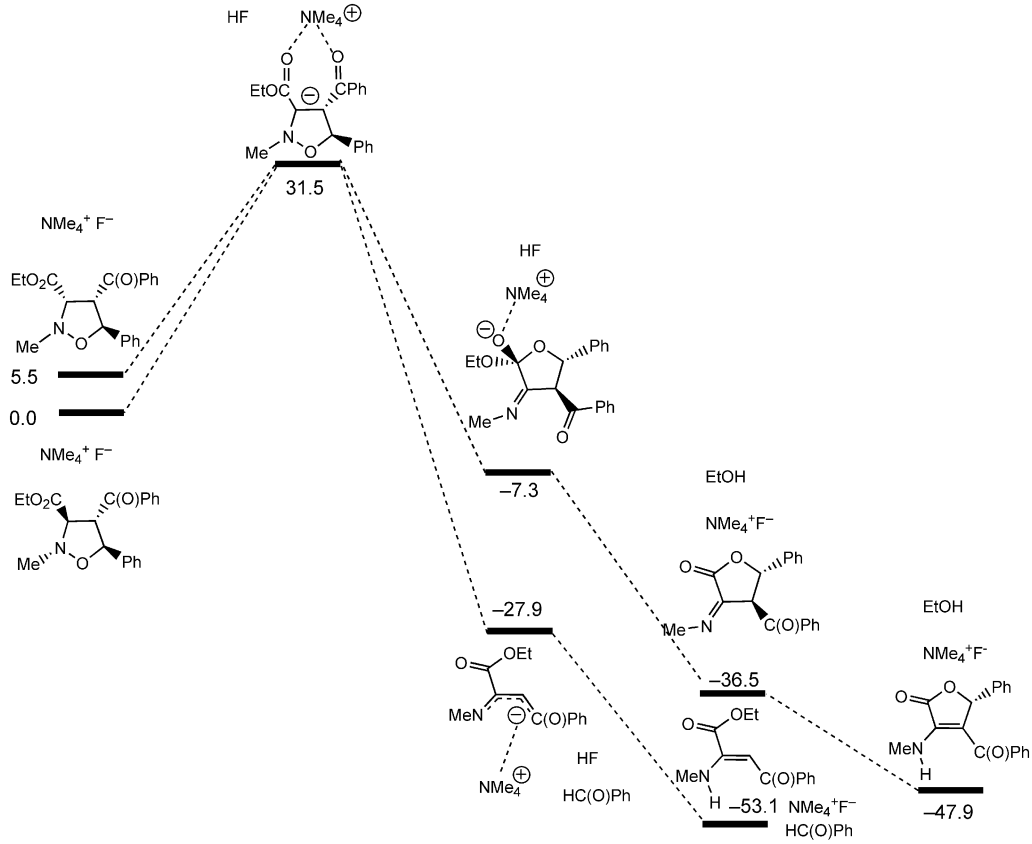

Figure 8. Gibbs free-energy diagram [kcal/mol] for the two competitive reactions of compound **11**. Data from full geometry B3LYP/6-31+G(d,p) optimizations in THF. Only initial reagents, final products, and stable intermediates are reported.

tant feature for both **13-II** and **11-II** contact ion pairs is observed when the countercation is located in front of the N–O bond of the isoxazolidine ring (Figure 7).

In this case, the structure that carries a negative charge on the oxygen atom is largely stabilized; the N–O bond breaks and rotations around C^3–C^4 and C^4–C^5 bonds can occur, leading to the subsequent intramolecular lactonization. These results clearly indicate that the countercation has a pivotal role in the stability of the various structures for the isoxazolidine anion, thus modulating the two competitive reaction channels.

Energetics for stable intermediates and final products for the aldehyde elimination or intramolecular lactonization are reported in Figures 8 and 9 for compounds **11** and **13**, respectively. Related optimized structures are reported in the Supporting Information (see Figures S3 and S4 in the Supporting Information).

The energy curves for the two reaction channels are similar. Hydrogen abstraction by $(CH_3)_4N^+F^-$, leading to the formation of the contact ion pair **II**, is highly endoergonic for both analyzed compounds. Subsequent reaction pathways are largely exoergonic and hence irreversible. The aldehyde elimination seems thermodynamically favored for isoxazolidine **11** because of the large energy released in fragmentation of the sterically hindered isoxazolidine ring. Conversely, the lactonization process is thermodynamically favored for compound **13**.

Beyond the thermodynamic aspects, it is also important to scrutinize energetic and structural evolution of intermediate contact ion pairs **II** towards the formation of the two competitive **III** and **VI** intermediates. The energy profile for the formation of these intermediates has been constructed by using the N^2–C^3–C^4–C^5 torsional angle as a "reaction coordinate" (Figure 10). The energy curves are rather flat in the early stages of the rotation with a shallow maximum in both senses of rotation. For a rotation greater than 20° in both directions with respect to the equilibrium position in **11-II**, highly steric demanding phenyls at the C^4- and C^5-positions move towards the counteraction, which is subsequently forced to move far away. Thus, the ionic stabilization is reduced and the isoxazolidine ring increases its negative charge resulting in a spontaneous retroaldolization with formation of **11-VI** ($\Delta G^{\ddagger}$ = 1.2 kcal/mol; see Figure S5 in the Supporting Information for the transition-state structure).

For the **13-II** contact ion pair, rotations around the C^3–C^4 bond result in a very different behavior because of the absence of sterically demanding substituents at positions C^4 and C^5 of the isoxazolidine ring. Upon rotations greater than 20° from the equilibrium position, in both directions, the $(CH_3)_4N^+$ countercation undergoes large displacements and synchronously the C^4–C^5 bond undergoes large rotations to approach the countercation to the O^1, with the consequent opening of the heterocyclic system. The activation

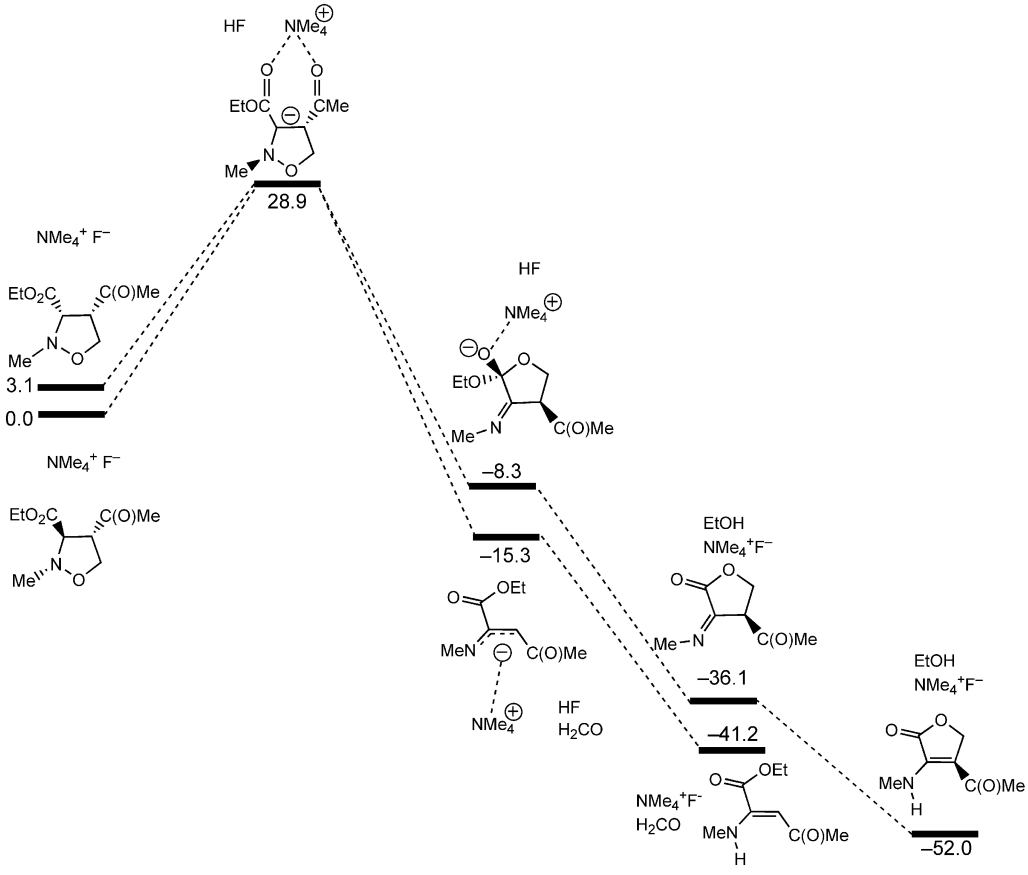

Figure 9. Gibbs free-energy diagram [kcal/mol] for the two competitive reactions of **13**. Data from full geometry B3LYP/6-31+G(d,p) optimizations in THF. Only initial reagents, final products, and stable intermediates are reported.

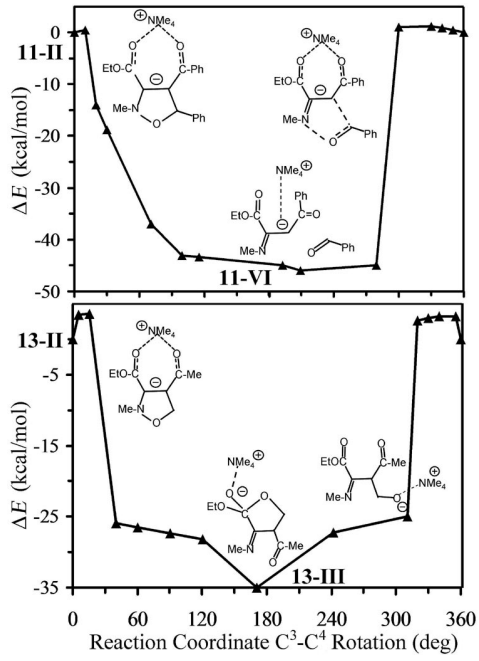

Figure 10. Electronic energy profile for rotation around C^3–C^4 in the **11-II** and **13-II** contact ion pairs. Data from full geometry B3LYP/6-31+G(d,p) optimizations in THF. Selected geometries showing important structural evolutions. The energy and N^2–C^3–C^4–C^5 torsional bond angle of contact ion pairs **13-II** and **11-II** have been assumed as references.

free energy for this process is 2.7 kcal/mol (see Figure S6 in the Supporting Information for a transition-state structure). As the C^3–C^4 bond is rotated by 180 ± 20°, the nucleophilic $–O^{1-}$ group approaches the carboxyethyl and lactonization occurs.

We have also quantified the energy barrier for the competitive aldehyde extrusion in the **13-II** contact ion pair. The energy profile has been constructed by using the O^1–N^2 bond length as the "reaction coordinate" (Figure 11). The energy increases quickly upon the O^1–N^2 bond lengthening and reaches the maximum at 1.73 Å, for which a transition-state structure was found with an activation free energy of 3.1 kcal/mol (see Figure S5 in the Supporting Information for the transition-state structure). After that, a profound structural rearrangement occurs and the intermediate **13-VI** together with formaldehyde are produced.

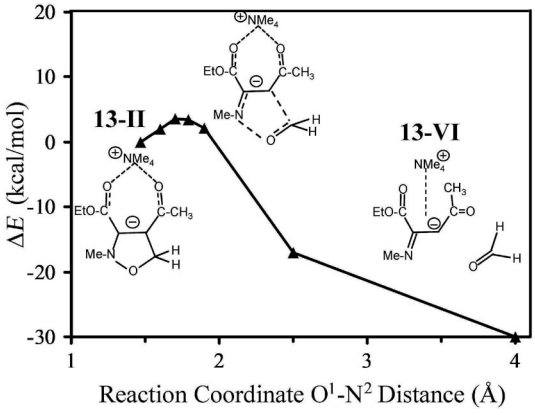

Figure 11. Electronic energy profile for aldehyde extrusion from the **13-II** contact ion pair along the O^1–N^2 reaction coordinate. Data from full geometry B3LYP/6-31+G(d,p) optimizations in THF. Selected geometries showing important structural evolutions are reported.

According to these theoretical data, the retroaldolization is thermodynamically and kinetically favored for isoxazolidine **11**, whereas, on the contrary, the lactonization is thermodynamically and kinetically favored for isoxazolidine **13**. These results are in full agreement with the experimental evidence and can be used also to rationalize the data obtained for related isoxazolidines **10**, **12**, and **14** (Table 2). Thus, by starting from the less substituted isoxazolidine **13**, the replacement in the isoxazolidine ring of H with CH_3 at C^5 and COMe with CO_2Me at C^4 (**14**) does not produce a significant change in the ratio of the final products and lactones are exclusively formed. Upon increasing markedly the steric hindrance of the substituents (phenyl group at C^4 or C^5 centers as in **10** and **12**), the alternative route becomes competitive and only 20% of the lactone is formed.

When steric hindrance in both C^4 and C^5 centers further increases (compound **11**), the thermodynamic drive toward aldehyde extrusion is maximized and countercation mobility is minimized and hence the β-enaminone is exclusively formed.

Conclusions

A new reaction pathway of 3-alkoxycarbonyl-4-acyl- or 3,4-dialkoxycarbonyl-substituted isoxazolidines **10**–**12** to β-enaminones **5**, by treatment with TBAF is reported. This reaction channel competes with the route leading to 3-methylamino-2(5*H*)-furanones **4**, according to the nature of the substituents at C^4 and C^5. The mechanistic rationalization of this new pathway has been performed according to a computational study, which has allowed us to understand the factors that ultimately control the competitive reaction routes.

All the relevant elementary steps of the two alternative mechanisms (lactonization and retroaldolization) for two representative isoxazolidines **11** and **13** have been analyzed by quantum chemical methods. Any realistic theoretical modeling requires the explicit inclusion of countercation and solvent effects. Isoxazolidine ring activation by TBAF leads to the formation of stable **11-II** and **13-II** contact ion pairs that are the starting point of both reaction channels. The oxygen atoms of carboxyl groups at the C^3 and C^4 positions chelate the countercation and successive dynamics determine the final pathways. The retroaldolization occurs preferentially because of the steric strain posed by the largely hindered ring substituents in **11-II**, which prevents the possibility of the countercation passing from one side to the other side of the isoxazolidine ring to stabilize the alkoxy anion **II′** (Figure 4). Conversely, the reduced size of the ring substituents for **13-II** decreases the repulsive interactions and, hence, the intrinsic tendency toward ring fragmentation. Furthermore, the mobility of countercation is

highly permitted and can assist rotation around C^3–C^4 and C^4–C^5 for the competitive lactonization.

In general, the relative importance of the two reaction channels may be predicted by considering the electronic and steric features of substituents on the isoxazolidine ring.

Experimental Section

Computational Details: Computations were performed at the density functional level employing the hybrid B3LYP functional with the 6-31+G** basis set. The geometries were optimized by using standard gradient techniques within the restricted Hartree–Fock formalism and including explicitly solvent effects. The "distinguished reaction coordinate" procedure has been used to analyze the full progress of the lactonization and retroaldolization occurring in intermediates **11-II** and **13-II**. The geometry optimization of the first point was begun from the ground-state structure of **11-II** and **13-II** contact ion pairs. As the reaction proceeds, the starting structure in each geometry optimization was taken from the immediately preceding point. Once the approximate transition-state structure was determined, the true transition state was refined by using the second derivatives of the energy techniques. All stationary points presently characterized by vibrational analysis are true minima or true transition states (no imaginary frequency and only one imaginary frequency, respectively).

The computed energies were corrected for zero-point vibrational and thermal energies and entropies to obtain free-energy changes ($\Delta G°_{298}$) at 298 K. Solvent effects were modeled by using the polarized continuum method (PCM) adopting a 7.64 dielectric constant for THF solvent as implemented in the G09 program.[11]

Methods: Solvents and reagents were used as received from commercial sources. Melting points were determined with a Kofler apparatus and are reported uncorrected. Elemental analyses were performed with a Perkin–Elmer elemental analyzer. NMR spectra (^{1}H NMR recorded at 500 MHz, ^{13}C NMR recorded at 125 MHz) were obtained on Varian Instruments and are referenced in ppm relative to TMS or the solvent signal. Mass spectroscopy data were collected on an HRMS-EI. Thin-layer chromatographic separations were performed on Merck silica gel 60-F_{254} precoated aluminum plates. Flash chromatography was accomplished on Merck silica gel (200–400 mesh). Preparative separations were carried out by a MPLC Büchi C-601 by using Merck silica gel 0.040–0.063 mm and the eluting solvents were delivered by a pump at the flow rate of 3.5–7.0 mL min^{-1}. The identification of samples from different experiments was secured by mixed melting points and superimposable NMR spectra. (*E*)- and (*Z*)-*C*-(ethoxycarbonyl)-*N*-methyl-nitrones **6** were prepared according to described procedures.[12]

General Procedure for the Synthesis of Isoxazolidines 10a,b: A solution of nitrone **6** (1 g, 7.6 mmol) and methyl *trans*-cinnamate **7** (1.84 g, 11.4 mmol) in dry toluene (20 mL) was heated at 80 °C for 18 h. The mixture was evaporated and the resulting residue was purified by MPLC on a silica gel with cyclohexane/ethyl acetate (80:20) to afford a mixture of regioisomers **10a** and **10b** in a 4.5:1 ratio.

3-Ethyl 4-Methyl (3S*R*,4*SR*,5*SR*)-2-Methyl-5-phenylisoxazolidine-3,4-dicarboxylate (10a): R_f = 0.52. Colorless oil (1.55 g, 69.6%). ^{1}H NMR ($CDCl_3$, 500 MHz): δ = 1.29 (t, J = 8.0 Hz, 3 H, CH_3), 2.94 (s, 3 H, N-CH_3), 3.82 (s, 3 H, OCH_3), 3.89 (dd, J = 5.0 and 7.0 Hz, 1 H, 4-H), 4.03 (d, J = 5.0 Hz, 1 H, 3-H), 4.28 (q, J = 8.0 Hz, 2 H, O-CH_2), 5.39 (d, J = 7.0 Hz, 1 H, 5-H), 7.24–7.48 (m, 5 H, Ar) ppm. ^{13}C NMR (125 MHz, $CDCl_3$): δ = 14.1, 52.6, 56.1, 59.2, 61.8, 74.2, 81.3, 126.8, 128.4, 128.6, 138.3, 169.6, 171.7 ppm. HRMS (EI): calcd. for $C_{15}H_{19}NO_5$ $[M]^+$ 293.1263; found 293.1265. $C_{15}H_{19}NO_5$ (293.32): calcd. C 61.42, H 6.53, N 4.78; found C 61.38, H 6.49, N 4.72.

3-Ethyl 4-Methyl (3S*R*,4*RS*,5*RS*)-2-Methyl-5-phenylisoxazolidine-3,4-dicarboxylate (10b): R_f = 0.48. Colorless oil (0.343 g, 15.4%). ^{1}H NMR ($CDCl_3$, 500 MHz): δ = 1.30 (t, J = 7.0 Hz, 3 H, CH_3), 2.91 (s, 3 H, N-CH_3), 3.66 (dd, J = 3.5, 7.0 Hz, 1 H, 4-H), 3.71 (s, 3 H, OCH_3), 3.77 (d, J = 3.5 Hz, 1 H, 3-H), 4.21 (q, J = 7.0 Hz, 2 H, O-CH_2), 5.34 (d, J = 7.0 Hz, 1 H, 5-H), 7.28–7.47 (m, 5 H, Ar) ppm. ^{13}C NMR ($CDCl_3$, 125 MHz): δ = 14.1, 52.3, 56.5, 58.2, 62.1, 74.2, 81.5, 126.9, 127.7, 128.6, 139.5, 168.3, 170.3 ppm. HRMS (EI): calcd. for $C_{15}H_{19}NO_5$ $[M]^+$ 293.1263; found 293.1259. $C_{15}H_{19}NO_5$ (293.32): calcd. C 61.42, H 6.53, N 4.78; found C 61.37, H 6.45, N 4.81.

General Procedure for the Synthesis of Isoxazolidines 11a,d and 12a–c: Trimethylaluminum (0.2 mL, 2 M solution in toluene) was added to a solution of 2,6-diphenylphenol (290 mg, 0.38 mmol) in dry dichloromethane (20 mL) at 0 °C under a N_2 atmosphere and the solution was left stirring for 30 min at this temperature. Then, alkene **8** or **9** (3.8 mmol) was added at 0 °C and, after 30 min, a solution of nitrone **6** (3.8 mmol in 10 mL of CH_2Cl_2) was added dropwise over 20 min. The reaction mixture was stirred for 18 h at room temperature. Then, the mixture was filtered through a Celite pad, the filtrate was evaporated in vacuo, and the residue subjected to medium pressure liquid chromatography (MPLC) by using cyclohexane/ethyl acetate (9:1) as the eluent. The reaction of nitrone **6** and (*E*)-chalcone **8** affords a mixture of stereoisomers **11a**–**d** (yield 86%), whereas the reaction of nitrone **6** and (*E*)-1-phenylbut-2-en-1-one (**9**) affords a mixture of stereoisomers **12a**–**c** (yield 85%).

Ethyl (3*SR*,4*SR*,5*SR*)-5-Benzoyl-2-methyl-4-phenylisoxazolidine-3-carboxylate (11c): R_f = 0.50. Colorless oil (0.159 g, 12.4%). ^{1}H NMR ($CDCl_3$, 500 MHz): δ = 0.85 (t, J = 7.0 Hz, 3 H, CH_3), 2.92 (s, 3 H, NCH_3), 3.75 (d, J = 8.6 Hz, 1 H, 3-H), 3.79 (q, J = 7.0 Hz, 2 H, OCH_2), 4.43 (dd, J = 5.5, 8.6 Hz, 1 H, 4-H), 5.44 (d, J = 5.5 Hz, 1 H, 5-H), 7.31–7.94 (m, 10 H, Ar) ppm. ^{13}C NMR ($CDCl_3$, 125 MHz): δ = 13.6, 45.0, 54.1, 60.8, 74.6, 85.7, 127.7, 128.5, 128.6, 129.0, 129.4, 133.8, 138.1, 134.6, 167.9, 194,5 ppm. HRMS (EI): calcd. for $C_{20}H_{21}NO_4$ $[M]^+$ 339.1471; found 339.1476. $C_{20}H_{21}NO_4$ (339.39): calcd. C 70.78, H 6.24, N 4.13; found C 70.75, H 6.21, N 4.16.

Ethyl (3*SR*,4*RS*,5*RS*)-5-Benzoyl-2-methyl-4-phenylisoxazolidine-3-carboxylate (11d): R_f = 0.45. Colorless oil (0.158 g, 12.3%). ^{1}H NMR ($CDCl_3$, 500 MHz): δ = 1.23 (t, J = 7.5 Hz, 3 H, CH_3), 2.92 (s, 3 H, NCH_3), 3.45 (d, J = 8.0 Hz, 1 H, 3-H), 4.17 (q, J = 7.5 Hz, 2 H, OCH_2), 4.69 (dd, J = 5.0, 8.0 Hz, 1 H, 4-H), 5.17 (d, J = 5.0 Hz, 1 H, 5-H), 7.28–7.97 (m, 10 H, Ar) ppm. ^{13}C NMR ($CDCl_3$, 125 MHz): δ = 13.6, 44.7, 54.2, 61.5, 74.3, 85.9, 127.6, 128.0, 128.3, 129.0, 129.4, 133.2, 134.8, 144.7, 168.6, 196.2 ppm. HRMS (EI): calcd. for $C_{20}H_{21}NO_4$ $[M]^+$ 339.1471; found 339.1474. $C_{20}H_{21}NO_4$ (339.39): calcd. C 70.78, H 6.24, N 4.13; found C 70.79, H 6.25, N 4.10.

Ethyl (3*SR*,4*RS*,5*RS*)-4-Benzoyl-2-methyl-5-phenylisoxazolidine-3-carboxylate (11b): R_f = 0.40. Colorless oil (0.158 g, 12.3%). ^{1}H NMR ($CDCl_3$, 500 MHz): δ = 1.27 (t, J = 7.0 Hz, 3 H, CH_3), 3.00 (s, 3 H, NCH_3), 4.15 (d, J = 5.5 Hz, 1 H, 3-H), 4.27 (q, J = 7.0 Hz, 2 H, OCH_2), 4.85 (dd, J = 5.0, 7.5 Hz, 1 H, 4-H), 5.42 (d, J = 7.5 Hz, 1 H, 5-H), 7.31–7.74 (m, 10 H, Ar) ppm. ^{13}C NMR ($CDCl_3$, 125 MHz): δ = 14.1, 46.7, 61.9, 62.1, 82.8, 127.3, 128.0, 128.3, 128.6, 128.7, 133.8, 136.0, 137.8, 170.5, 197.3 ppm. HRMS (EI): calcd. for $C_{20}H_{21}NO_4$ $[M]^+$ 339.1471; found 339.1474.

$C_{20}H_{21}NO_4$ (339.39): calcd. C 70.78, H 6.24, N 4.13; found C 70.74, H 6.20, N 4.16.

Ethyl (3*SR*,4*SR*,5*SR*)-4-Benzoyl-2-methyl-5-phenylisoxazolidine-3-carboxylate (11a): R_f = 0.21. Colorless oil (0.632 g, 49%). ^{1}H NMR ($CDCl_3$, 500 MHz): δ = (t, J = 7.2 Hz, 3 H, CH_3), 2.90 (s, 3 H, NCH_3), 3.75 (d, J = 9.3 Hz, 1 H, 3-H), 3.92 (q, J = 7.2 Hz, 2 H, OCH_2), 4.51 (dd, J = 7.7, 9.3 Hz, 1 H, 4-H), 5.25 (d, J = 7.7 Hz, 1 H, 5-H), 7.22–7.64 (m, 10 H, Ar) ppm. ^{13}C NMR ($CDCl_3$, 125 MHz): δ = 13.7, 45.0, 60.6, 61.2, 73.0, 82.5, 126.9, 127.6, 128.4, 128.5, 128.6, 129.9, 133.4, 136.4, 168.2, 196.2 ppm. HRMS (EI): calcd for $C_{20}H_{21}NO_4$ $[M]^+$ 339.1471; found 339.1469. $C_{20}H_{21}NO_4$ (339.39): calcd. C 70.78, H 6.24, N 4.13; found C 70.73, H 6.26, N 4.10.

Ethyl (3*SR*,4*SR*,5*SR*)-5-Benzoyl-2,4-dimethylisoxazolidine-3-carboxylate (12c): R_f = 0.45. Light-yellow oil (0.081 g, 7.7%). ^{1}H NMR ($CDCl_3$, 500 MHz): δ = 1.35 (t, J = 7.0 Hz, 3 H, CH_3), 1.42 (d, J = 7.5 Hz, 3 H, CH_3), 2.90 (s, 3 H, NCH_3), 3.08 (d, J = 8.5 Hz, 1 H, 3-H), 3.52 (ddq, J = 5.5, 7.5, 8.5 Hz, 1 H, 4-H), 4.27 (q, J = 7.0 Hz, 2 H, OCH_2), 4.75 (d, J = 5.5 Hz, 1 H, 5-H), 7.44–8.15 (m, 5 H, Ar) ppm. ^{13}C NMR ($CDCl_3$, 125 MHz): δ = 11.2, 14.2, 44.3, 44.8, 61.0, 73.3, 82.1, 128.2, 128.8, 133.6, 138.0, 169.2, 197.2 ppm. HRMS (EI): calcd. for $C_{15}H_{19}NO_4$ $[M]^+$ 277.1314; found 277.1319. $C_{15}H_{19}NO_4$ (277.32): calcd. C 64.97, H 6.91, N 5.05; found C 64.99, H 6.88, N 5.09.

Ethyl (3*SR*,4*RS*,5*SR*)-4-Benzoyl-2,5-dimethylisoxazolidine-3-carboxylate (12b): R_f = 0.40. Light-yellow oil (0.161 g, 15.3%). ^{1}H NMR ($CDCl_3$, 500 MHz): δ = 0.99 (d, J = 6.5 Hz, 3 H, CH_3), 1.22 (t, J = 7.0 Hz, 3 H, CH_3), 2.94 (s, 3 H, NCH_3), 4.05 (d, J = 6.5 Hz, 1 H, 3-H), 4.19 (q, J = 7.0 Hz, 2 H, OCH_2), 4.59 (dq, J = 6.5, 8.5 Hz, 1 H, 5-H), 4.75 (dd, J = 6.5, 8.5 Hz, 1 H, 4-H), 7.26–7.96 (m, 5 H, Ar) ppm. ^{13}C NMR ($CDCl_3$, 125 MHz): δ = 14.3, 17.7, 46.4, 57.0, 62.4, 72.1, 74.7, 128.8, 128.9, 133.5, 138.9, 169.7, 196.8 ppm. HRMS (EI): calcd. for $C_{15}H_{19}NO_4$ $[M]^+$ 277.1314; found 277.1316. $C_{15}H_{19}NO_4$ (277.32): calcd. C 64.97, H 6.91, N 5.05; found C 64.95, H 6.89, N 5.02.

Ethyl (3*SR*,4*SR*,5*RS*)-4-Benzoyl-2,5-dimethylisoxazolidine-3-carboxylate (12a): R_f = 0.38. Light-yellow oil (0.053 g, 62%). ^{1}H NMR ($CDCl_3$, 500 MHz): δ = 0.98 (t, J = 6.0 Hz, 3 H, CH_3), 1.43 (d, J = 6.0 Hz, 3 H, CH_3), 2.86 (s, 3 H, NCH_3), 3.61 (d, J = 9.5 Hz, 1 H, 3-H), 3.97 (q, J = 6.0 Hz, 2 H, OCH_2), 4.18 (dd, J = 7.5, 9.5 Hz, 1 H, 4-H), 4.40 (dq, J = 6.0, 7.5 Hz, 1 H, 5-H), 7.44–7.92 (m, 5 H, Ar) ppm. ^{13}C NMR ($CDCl_3$, 125 MHz): δ = 14.0, 17.8, 46.3, 57.3, 62.0, 71.5, 76.0, 128.4, 128.9, 137.8, 139.0, 169.4, 196.9 ppm. HRMS (EI): calcd. for $C_{15}H_{19}NO_4$ $[M]^+$ 277.1314; found 277.1317. $C_{15}H_{19}NO_4$ (277.32): calcd. C 64.97, H 6.91, N 5.05; found C 64.94, H 6.88, N 5.03.

General Procedure for the Synthesis of 3-Amino-2(5*H*)-furanones 4a,b and β-Enaminones 5a,b: TBAF (1.1 mL, 1.1 mmol, 1 M in THF) was added to a solution of isoxazolidine **10**–**12** (1 mmol) in dry THF (10 mL) and the mixture was stirred at 50 °C for 3 h. At the end of this time, the solvent was removed and the residue was purified by MPLC by using $CHCl_3$/MeOH (99:1) as the eluent.

Methyl 4-(Methylamino)-5-oxo-2-phenyl-2,5-dihydrofuran-3-carboxylate (4a): Colorless oil (0.034 g, 18%) from **10a** or **10b** (293 mg). ^{1}H NMR ($CDCl_3$, 500 MHz): δ = 3.36 (d, J = 5.5 Hz, 3 H, NCH_3), 3.61 (s, 3 H, OCH_3), 5.95 (s, 1 H, 5-H), 6.54 (br. s, 1 H, NH) 7.27–7.36 (m, 5 H, Ar) ppm. ^{13}C NMR ($CDCl_3$, 125 MHz): δ = 30.0, 80.8, 107.9, 127.3, 128.5, 12.0, 144.4, 163.5, 168.9 ppm. HRMS (EI): calcd. for $C_{13}H_{13}NO_4$ $[M]^+$ 247.0845; found 247.0848. $C_{13}H_{13}NO_4$ (247.25): calcd. C 63.15, H 5.30, N 5.67; found C 63.12, H 5.32, N 5.65.

1-Ethyl 4-Methyl 2-(Methylamino)fumarate (5a): Light-yellow oil (0.135 g, 72%) from **10a** or **10b** (293 mg). ^{1}H NMR ($CDCl_3$, 500 MHz): δ = 1.33 (t, J = 7.2 Hz, 3 H, CH_3), 3.02 (d, J = 5.2 Hz, 3 H, NCH_3), 3.69 (s, 3 H, OCH_3), 4.34 (q, J = 7.2 Hz, 2 H, OCH_2), 5.22 (s, 1 H, CH=), 7.99 (br. s, 1 H, NH) ppm. ^{13}C NMR ($CDCl_3$, 125 MHz): δ = 21.4, 26.8, 45.2, 75.9, 117.9, 142.5, 167.0, 193.1 ppm. HRMS (EI): calcd. for $C_8H_{13}NO_4$ $[M]^+$ 187.0845; found 187.0842. $C_8H_{13}NO_4$ (187.20): calcd. C 51.33, H 7.00, N 5.48; found C 51.30, H 7.04, N 5.46.

4-Benzoyl-5-methyl-3-(methylamino)furan-2(5*H*)-one (4b): Colorless oil (42 mg, 18%) from **12a** or **12b** (277 mg). ^{1}H NMR ($CDCl_3$, 500 MHz): δ = 1.40 (d, J = 4.5 Hz, 3 H, CH_3), 3.20 (d, J = 3.5 Hz, 3 H, NCH_3), 5.05 (q, J = 4.5 Hz, 1 H, 5-H), 6.70 (br. s, NH), 7.40–7.90 (m, 5 H, Ar) ppm. ^{13}C NMR ($CDCl_3$, 125 MHz): δ = 18.2, 31.2, 51.9, 75.0, 110.6, 146.7, 162.6, 170.6 ppm. HRMS (EI): calcd. for $C_{13}H_{13}NO_3$ $[M]^+$ 231.0895; found 231.0893. $C_{13}H_{13}NO_3$ (231.25): calcd. C 67.52, H 5.67, N 6.02; found C 67.50, H 5.66, N 6.00.

(*Z*)-Ethyl 2-(Methylamino)-4-oxo-4-phenylbut-2-enoate (5b): Yellow oil (200 mg, 90%) from **11a** or **11b** (339 mg); (167 mg, 72%) from **12a** or **12b** (277 mg). ^{1}H NMR ($CDCl_3$, 500 MHz): δ = 1.35 (t, J = 7.3 Hz, 3 H, CH_3), 3. 12 (d, J = 5.5 Hz, 3 H, NCH_3), 4.36 (q, J = 7.3 Hz, 2 H, OCH_2), 6.01 (s, 1 H, CH=), 7.5–8.1 (m, 5 H, Ar), 10.75 (br. s, 1 H, NH) ppm. ^{13}C NMR ($CDCl_3$, 125 MHz): δ = 14.8, 32.4, 62.8, 92.3, 127.2, 128.2, 131.8, 140.3, 154.8, 164.0, 191.5 ppm. HRMS (EI): calcd. for $C_{13}H_{15}NO_3$ $[M]^+$ 233.1052; found 233.1058. $C_{13}H_{15}NO_3$ (233.27): calcd. C 66.94, H 6.48, N 6.00; found C 66.91, H 6.45, N 6.05.

Supporting Information (see also the footnote on the first page of this article): Additional figures, NMR characterization of compounds **10**–**12**, computed structures for high lying minima and transition states, Cartesian coordinates and NMR spectra of compounds **4**, **5**, **10**–**12**.

Acknowledgments

We gratefully acknowledge the Ministero dell'Università e della Ricerca (MIUR) (Progetto Nazionale 2008–2010: Amminoacidi conformazionalmente rigidi: versatili building blocks per la sintesi regio- e stereoselettiva di nuovi sistemi policiclici catalizzata da metalli di transizione; Progettazione e sintesi stereoselettiva di composti eterociclici quali nuovi agenti antivirali) and the University of Catania and Messina for their generous support of this work.

[1] a) C.-H. Tan, A. B. Holmes, *Chem. Eur. J.* **2001**, *7*, 1845–1854; A. Brandi, F. Cardona, S. Cicchi, F. M. Cordero, A. Goti, *Chem. Eur. J.* **2009**, *15*, 7808–7821; b) U. Chiacchio, A. Padwa, G. Romeo, *Curr. Org. Chem.* **2009**, *13*, 422–447; c) S. M. Lait, D. A. Rankic, B. A. Keay, *Chem. Rev.* **2007**, *107*, 767–796; d) G. Singh, M. P. S. Ishar, V. Gupta, M. Kalyan, S. S. Bhella, *Tetrahedron* **2007**, *73*, 4773–4778; e) G. Pandey, P. Banerjee, R. Gadre, *Chem. Rev.* **2006**, *106*, 4484–4517; f) U. Chiacchio, A. Rescifina, M. G. Saita, D. Iannazzo, G. Romeo, J. A. Mates, T. Tejero, P. Merino, *J. Org. Chem.* **2005**, *70*, 899–9001; g) P. Merino, in: *Science of Synthesis*, Houben-Weyl Methods of Molecular Transformations (Ed.: A. Padwa), Thieme, Stuttgart, **2004**, pp. 511–580; h) A. R. Minter, B. B. Brennan, A. K. Mapp, *J. Am. Chem. Soc.* **2004**, *126*, 10504–10505; i) A. Padwa, W. H. Pearson, in: *Synthetic Applications of 1,3-Dipolar Cycloaddition Chemistry towards Heterocycles and Natural Products*, John Wiley & Sons, Hoboken, N. J., **2003**, vol. 2, pp. 539–621; j) Tejero, U. Chiacchio, G. Romeo, D. Iannazzo, R. Romeo, P. Merino, J. A. Mates, J. Revuelta, *Tetrahedron: Asymmetry*

2002, *13*, 173–190; k) U. Chiacchio, A. Corsaro, V. Pistarà, A. Rescifina, D. Iannazzo, A. Piperno, G. Romeo, R. Romeo, G. Grassi, *Eur. J. Org. Chem.* **2002**, 1206–1212; l) U. Chiacchio, A. Corsaro, A. Rescifina, M. Bkaithan, A. Piperno, T. Privitera, G. Romeo, *Tetrahedron* **2001**, *57*, 3425–3433; m) U. Chiacchio, A. Corsaro, D. Iannazzo, A. Piperno, A. Rescifina, R. Romeo, G. Romeo, *Tetrahedron Lett.* **2001**, *42*, 1777–1780; n) U. Chiacchio, A. Rescifina, G. Romeo, in: *Targets in Heterocyclic Systems. Chemistry and Properties* (Eds.: O. Attanasi, D. Spinelli), Italian Society of Chemistry, **1997**, vol. 1, pp. 225–276.

[2] a) T. B. Nguyen, A. Beauseigneur, A. Martel, R. Dhal, M. Laurent, G. Dujardin, *J. Org. Chem.* **2010**, *75*, 611–620; b) A. Bădoiu, Y. Brinkmann, F. Viton, E. P. Künding, *Pure App. Chem.* **2008**, *80*, 1013–1018; c) T. B. Nguyen, A. Martel, R. Dhal, G. Dujardin, *J. Org. Chem.* **2008**, *73*, 2621–2632; d) R. Romeo, D. Iannazzo, A. Piperno, M. A. Chiacchio, *Eur. J. Org. Chem.* **2005**, 2368–2373; e) G. Romeo, D. Iannazzo, A. Piperno, R. Romeo, A. Corsaro, A. Rescifina, U. Chiacchio, *Mini-Rev. Org. Chem.* **2005**, *2*, 59–77; f) P. Merino, *Compt. Rend. Chim.* **2005**, *8*, 775–788; g) U. Chiacchio, A. Piperno, A. Rescifina, G. Romeo, N. Uccella, *Tetrahedron* **1998**, *54*, 5695–5708; h) F. Casuscelli, M. R. Di Bella, R. Ficarra, S. Melardi, G. Romeo, U. Chiacchio, A. Rescifina, *Gazz. Chim. It.* **1997**, *127*, 367–371; i) U. Chiacchio, A. Liguori, G. Romeo, G. Sindona, N. Uccella, *Heterocycles* **1993**, *36*, 799–817; j) S. Cicchi, A. Goti, A. Brandi, A. Guarna, F. De Sarlo, *Tetrahedron Lett.* **1990**, *31*, 3351–3354; k) J. W. Grate, G. C. Frye, in: *Sensors Update* (Eds.: H. Baltes, W. Göpel, J. Hesse), Wiley-VCH, Weinheim, **1996**, vol. 2, pp. 10–20.

[3] J. Ariza, J. Font, R. M. Ortuno, *Tetrahedron Lett.* **1991**, *32*, 1979–1982.

[4] a) U. Chiacchio, D. Iannazzo, A. Piperno, V. Pistarà, A. Rescifina, G. Romeo, R. Romeo, *Tetrahedron* **2004**, *60*, 6593–6596; b) U. Chiacchio, A. Corsaro, D. Iannazzo, A. Piperno, A. Procopio, A. Rescifina, G. Romeo, R. Romeo, *J. Org. Chem.* **2002**, *67*, 4380–4383; c) F. Casuscelli, U. Chiacchio, M. R. Di Bella, A. Rescifina, G. Romeo, R. Romeo, N. Uccella, *Tetrahedron* **1995**, *51*, 8605–8612.

[5] D. Iannazzo, A. Piperno, G. Romeo, R. Romeo, U. Chiacchio, A. Rescifina, E. Balestrieri, B. Macchi, A. Mastino, R. Cortese, *Bioorg. Med. Chem.* **2008**, *16*, 9610–9615.

[6] a) T. Persson, J. Nielsen, *Org. Lett.* **2006**, *8*, 3219–3222; b) Y. O. Ko, Y. S. Chun, C.-L. Park, Y. Kim, H. Shin, S. Ahn, J. H.-S. Lee, *Org. Biomol. Chem.* **2009**, *7*, 1132–1136.

[7] a) T. Hashimoto, M. Omote, K. Maruoka, *Org. Biomol. Chem.* **2008**, *6*, 2263–2265; b) U. Chiacchio, A. Corsaro, D. Iannazzo, A. Piperno, G. Romeo, R. Romeo, M. G. Saita, A. Rescifina, *Eur. J. Org. Chem.* **2007**, 4758–4764; c) P. Merino, T. Tejero, U. Chiacchio, G. Romeo, A. Rescifina, *Tetrahedron* **2007**, *63*, 1448–1458; d) K. R. R. Kumar, H. Mallesha, K. S. Rangappa, *Synth. Commun.* **2003**, *33*, 1545–1555; e) P. Merino, S. Franco, F. L. Merchan, T. Tejero, *J. Org. Chem.* **2000**, *65*, 5575–5589.

[8] S. Kanemasa, N. Ueno, M. Shirahase, *Tetrahedron Lett.* **2002**, *43*, 657–660.

[9] To better analyze these aspects, additional calculations have been performed by using an alternative BPW91-DFT parametrization and traditional ab initio MP2 methods with the 6-31+G(d,p) basis set and including solvent effects. The great tendency toward aldehyde elimination from "free" isoxazolidine derivatives is confirmed and, for example, **13-II** at the MP2 level formaldehyde expulsion releases more than 20 kcal/mol. Nevertheless, the thermodynamic drive for ring degradation is less pronounced when the traditional MP2 is used with respect to DFT-based methods.

[10] a) C.-Y. Liu, X. Wang, T. Furuyama, S. Yasuike, A. Muranaka, K. Morokuma, M. Uchiyama, *Chem. Eur. J.* **2010**, *16*, 1780–1784; b) G. Lanza, I. L. Fragalà, T. J. Marks, *J. Am. Chem. Soc.* **1998**, *120*, 8257–8258; c) G. Lanza, I. L. Fragalà, T. J. Marks, *J. Am. Chem. Soc.* **2000**, *122*, 12764–12777; d) G. Lanza, I. L. Fragalà, T. J. Marks, *Organometallics* **2002**, *21*, 5594–5612.

[11] *Gaussian 09*, Revision A.1, M. J. Frisch, G. W. Trucks, H. B. Schlegel, G. R. Scuseria, M. A. Robb, J. R. Cheeseman, G. Scalmani, V. Barone, B. Mennucci, G. A. Petersson, H. Nakatsuji, M. Caricato, X. Li, H. P. Hratchian, A. F. Izmaylov, J. Bloino, G. Zheng, J. L. Sonnenberg, M. Hada, M. Ehara, K. Toyota, R. Fukuda, J. Hasegawa, M. Ishida, T. Nakajima, Y. Honda, O. Kitao, H. Nakai, T. Vreven, J. A. Montgomery Jr., J. E. Peralta, F. Ogliaro, M. Bearpark, J. J. Heyd, E. Brothers, K. N. Kudin, V. N. Staroverov, R. Kobayashi, J. Normand, K. Raghavachari, A. Rendell, J. C, Burant, S. S. Iyengar, J. Tomasi, M. Cossi, N. Rega, N. J. Millam, M. Klene, J. E. Knox, J. B. Cross, V. Bakken, C. Adamo, J. Jaramillo, R. Gomperts, R. E. Stratmann, O. Yazyev, A. J. Austin, R. Cammi, C. Pomelli, J. W. Ochterski, R. L. Martin, K. Morokuma, V. G. Zakrzewski, G. A. Voth, P. Salvador, J. J. Dannenberg, S. Dapprich, A. D. Daniels, O. Farkas, J. B. Foresman, J. V. Ortiz, J. Cioslowski, D. J. Fox, Gaussian, Inc., Wallingford CT, **2009**.

[12] J. Hara, Y. Inouye, H. Kakisawa, *Bull. Chem. Soc. Jpn.* **1981**, *54*, 3871–3872.

Received: April 26, 2010
Published Online: September 10, 2010

